Journal of the European Ceramic Society **15** (1995) 377–383

0955-2219/95/$9.50

Bridging Stress Relations for Ceramic Materials

T. Fett,[a] and D. Munz[b]

[a] Forschungszentrum Karlsruhe, Postfach 3640, Institut für Materialforschung II, D-76021, Karlsruhe, Germany
[b] Universität Karlsruhe, Institut für Zuverlässigkeit und Schadenskunde im Maschinenbau, Karlsruhe, Germany

(Received 2 June 1994; revised version received 12 August 1994; accepted 22 August 1994)

Abstract

In ceramic materials, bridging stresses are generated in the wake of propagating cracks due to crack interactions. Such stresses can be caused by friction of sliding grains or by elastic interactions where the crack surface contact behaves like a spring. Both types of interactions are described and a model is proposed which allows us to combine the two effects.

1 Introduction

Coarse-grained Al_2O_3 shows an R–curve behaviour which is characterised by an increase in crack growth resistance with increasing crack extension. In the past it has been shown by experimental[1] and theoretical investigations[2] that the R–curve is not a unique material property. The shape of the curve depends on the geometry of the test specimens, the initial crack depth, the type of loading (tension, bending) and on the special type of crack extension (stable and subcritical crack propagation).

It was demonstrated experimentally[3–6] that this effect is caused by crack border interactions in the wake of the advancing crack. The bridging interactions were observed mainly in materials with large grains. The crack face interactions localised at single grains can transfer loads which can be modelled in a more homogeneous way by so-called bridging stresses σ_{br} which depend only on the crack opening displacement δ. The bridging stresses shield the crack tip from the external loads.

In the special case of R–curves caused by bridging effects, the relation between bridging stresses and crack opening displacement is a material property which is expected to be much less influenced by special test conditions. In the literature the bridging stresses are mostly considered to be caused by frictional effects.[7] This description is well established for coarse-grained Al_2O_3. In hot-pressed silicon nitride, bridging zones act more like elastic springs of limited extension.[8]

Recently, Dauskardt[9] found experimental evidence for a combination of frictional and elastic behaviour of bridging interactions in alumina.

It is the intention of this investigation to

- present a bridging relation for elastic bridging interactions taking into consideration a distribution for the maximum displacements at which the bridge fails and to
- describe a bridging model that exhibits the main features of load versus displacement curves as measured by Dauskardt.[9]

Therefore, in the first part of this investigation, bridging relations are described which are based on bridging interactions caused by friction and spring effects. In the second part a model is discussed which describes elastic and friction-induced response of crack surface interactions on crack opening displacements.

2 Bridging Relations

2.1 Relation for friction induced bridging stresses

For bridging stresses σ_{br} which are caused by friction effects, Mai and Lawn[7] proposed a relation

$$\sigma_{br,grain} = \begin{Bmatrix} \sigma_0(1-\delta/\delta_c)^m & \text{for } \delta/\delta_c<1 \\ 0 & \text{for } \delta/\delta_c>1 \end{Bmatrix} m=0,1,2,\ldots \quad (1)$$

as shown in Fig. 1(a) for m = 1. If we assume that the characteristic displacement for which the bridging stresses vanish is distributed like a Γ-distribution of first order[2] with a density $f(\delta_c)$

$$f(\delta_c) = \frac{1}{\delta_0}\frac{\delta_c}{\delta_0}\exp(-\delta_c/\delta_0) \quad (2)$$

then the macroscopically averaged bridging stresses result from

$$\sigma_{br,aver} = \int_0^\infty \sigma_{br,grain} f(\delta_c)\, d\delta_c \quad (3)$$

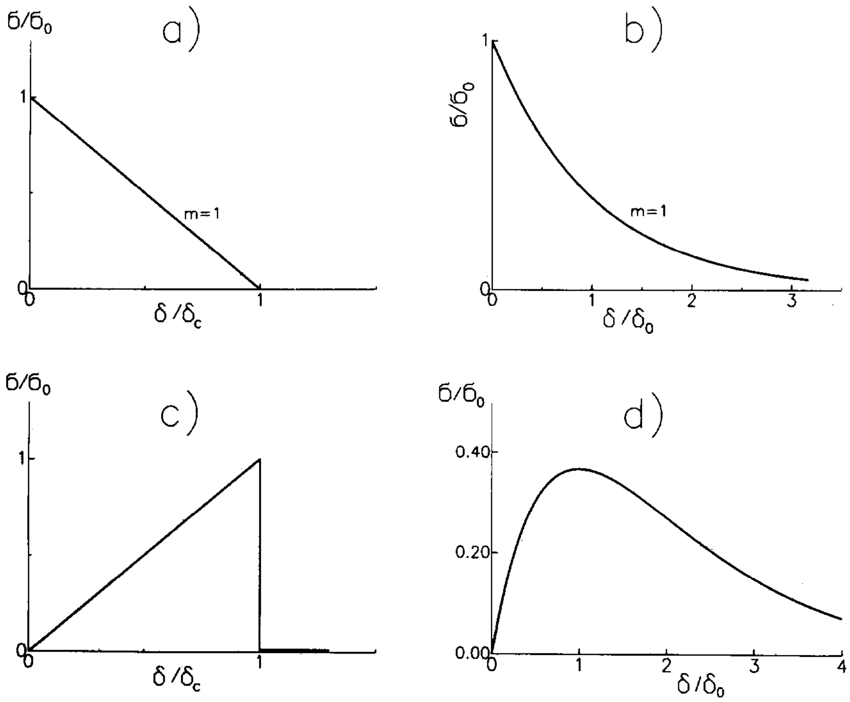

Fig. 1. Bridging stresses. (a) Local stress-displacement relation for frictional crack-surface interactions; (b) global stress-displacement relation for frictional crack-surface interactions; (c) local stress-displacement relation for a single spring; (d) global stress-displacement relation for spring-like crack-surface interactions.

For the mostly used case $m = 1$ the averaged bridging stress relation results

$$\sigma_{br,aver} = \sigma_0 \exp(-\delta/\delta_0) \tag{4}$$

as plotted in Fig. 1(b).

2.2 Bridging relations for springs with limited extensions

In case of spring-like stresses the bridging stresses in a single bridge may be expressed by

$$\sigma_{br,spring} = \begin{Bmatrix} \sigma_0\,\delta/\delta_c & \text{for } \delta/\delta_c<1 \\ 0 & \text{for } \delta/\delta_c>1 \end{Bmatrix} \tag{5}$$

with maximum extension δ_c and maximum stress σ_o, shown in Fig. 1(c).

Similar to the bridging effect it is assumed that the characteristic displacement δ_c for which the bridging stresses vanish is also Γ-distributed with a characteristical displacement value δ_0 characterising the 'width' of the distribution. The macroscopically averaged bridging stresses result from

$$\sigma_{br} = \int_0^\infty \sigma_{br,spring} f(\delta_c)\, d\delta_c \tag{6}$$

and one obtains by integration

$$\sigma_{br} = \sigma_0 \frac{\delta}{\delta_0} \exp(-\delta/\delta_0) \tag{7}$$

as given by Fig. 1(d). If we now assume a more narrow distribution of the values of δ_c's we can use the next higher order Γ-distribution, namely

$$f(\delta_c) = \frac{1}{\delta_0}\left(\frac{\delta_c}{\delta_0}\right)^2 \exp(-\delta_c/\delta_0) \tag{8}$$

and we obtain for the bridging-relation

$$\sigma_{br} = \sigma_0 \frac{\delta}{\delta_0}\left(1+\frac{\delta}{\delta_0}\right)\exp(-\delta/\delta_0) \tag{9}$$

For a comparison of eqns (7) and (9) see Fig. 11.

3 A Model for Frictional Bridging Stresses

In the following considerations a model is discussed that allows us to derive a relation for friction-induced bridging effects containing elastic components. As a first step the bridging effect is modelled as a two-dimensional problem for an internal crack in an infinite body, which is bridged by one single grain. In the second step a distribution of bridging grains is considered. In Fig. 2 a section

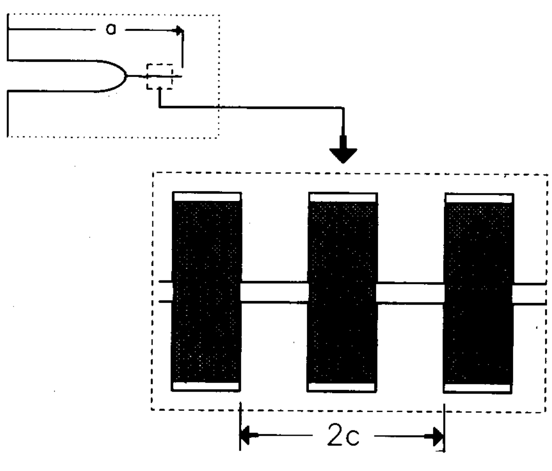

Fig. 2. Bridging model. A crack zone bridged by large grains.

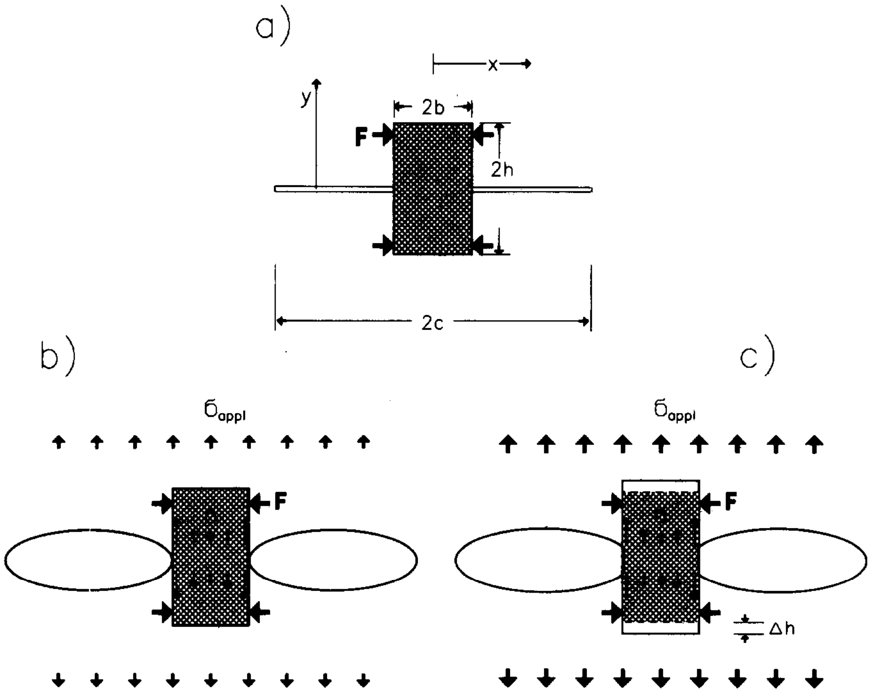

Fig. 3. Bridged crack. (a) Model of a bridged crack (unloaded). (b) Stresses and displacements for low remote loadings (schematic). (c) Stresses and displacements for high remote loadings (schematic).

of the bridged crack is shown. For the model the effect of one grain is considered and the problem can be treated as a crack of length $2c$ (twice the distance between two bridged grains). An elementary cell is shown in Fig. 3(a). Between the bridging grain and the surrounding material a residual stress acts due to mismatch of thermal expansion which creates the force F. This configuration is loaded by a remote stress $\sigma_{appl.}$ It is the aim of the following considerations to calculate the displacements at a remote location $y = y_0$ as a function of the applied stress. Figure 3(a) illustrates the geometry in the absence of externally applied stresses. For small, externally applied remote stresses σ_{appl} (Fig. 3(b)) the stresses and displacements are governed by the mixed boundary problem

$$\begin{aligned} \delta &= 0 \text{ for } |x| \le b \\ \sigma &= 0 \text{ for } |b| < |x| < |c| \end{aligned} \tag{10}$$

These conditions are valid until the load carried by the grain reaches the maximum friction force μF_0 between the bridging grain and its surroundings, i.e. for

$$2\int_0^b \sigma(x)\,\mathrm{d}x \le \mu F_0 \tag{11}$$

If the load carried by the grain exceeds μF_0, sliding between the bridging grain and the surroundings, with an amount Δh, occurs (Fig. 3(c)), the interaction force reduces to

$$F = F_0\,\frac{h - \Delta h}{h} \tag{12}$$

and the equilibrium condition of forces reads

$$2\int_0^b \sigma(x)\,\mathrm{d}x = \mu F_0 \frac{h - \Delta h}{h} \tag{13}$$

In this case, the boundary problem can be expressed by

$$\begin{aligned} \delta &= \Delta h \text{ for } |x| \le b \\ \sigma &= 0 \text{ for } |b| < |x| < |c| \end{aligned} \tag{14}$$

3.1 Calculation of displacements

Due to the symmetry of the problem with respect to $x = 0$, the computations can be restricted to positive values of x. Using the relation between stresses and displacements,[10] the mixed boundary problem can be written

$$\frac{1}{E'}\int_0^c \int_{\max(x,x')}^c h(c',x)h(c',x')\sigma(x')\mathrm{d}c'\mathrm{d}x' = \Delta h \tag{15}$$
$$\text{for } x \le b \qquad \sigma = 0 \qquad \text{for } b < x < c$$

The weight function for an internal crack in an infinite body under symmetrical load is[11]

$$h(x,c) = \frac{1}{\sqrt{\pi c}}\left[\left(\frac{c+x}{c-x}\right)^{1/2} + \left(\frac{c-x}{c+x}\right)^{1/2}\right] = \frac{2}{\sqrt{\pi c}}\,\frac{c}{\sqrt{c^2-x^2}} \tag{16}$$

In the absence of a bridging interaction the crack opening displacement field is given by

$$\delta_0(x) = \frac{2\sigma_{appl}}{E}\sqrt{c^2 - x^2} \tag{17}$$

The crack opening displacements caused by the stresses in the grain have to nullify these crack

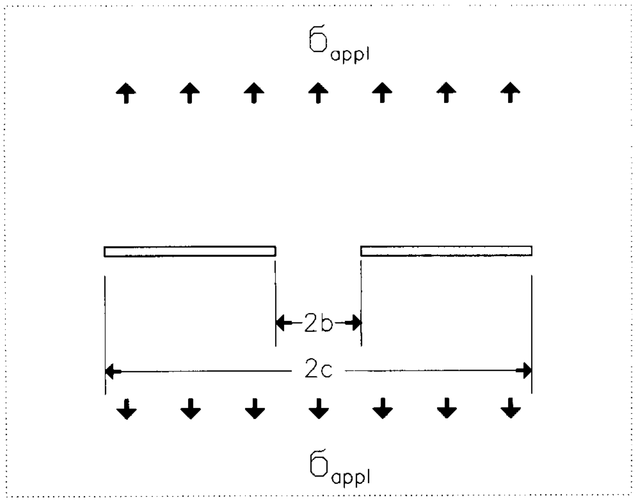

Fig. 4. Partial crack problem. Case 1: pair of collinear cracks.

opening displacements in the range $|x| \leq b$. So we have to solve

$$\frac{4}{E\pi}\int_x^c \frac{t}{\sqrt{t^2-x^2}}\left(\int_0^t \frac{\sigma(x)\,\mathrm{d}x}{\sqrt{t^2-x^2}}\right)\mathrm{d}t = -\frac{2}{E}\sigma_{\mathrm{appl}}\sqrt{c^2-x^2}+\Delta h \tag{18}$$

There are different possibilities of proceeding: (i) eqn (18) can be solved numerically; (ii) The displacement field can be superimposed by solutions existing for partial problems.

We will choose the second way here. As a first partial problem we compute the crack opening displacements for two neighbouring single cracks, Fig. 4, ensuring zero displacements within $|x| \leq b$. The crack opening displacements are (see for example[11])

$$\delta_1(x) = \frac{2\,c\,\sigma_{\mathrm{appl}}}{E'\boldsymbol{K}(k)}\left[\boldsymbol{K}(k)\,E(\varphi,k) - \boldsymbol{E}(k)\,F(\varphi,k)\right] \tag{19}$$

where $F(\varphi, k)$ and $E(\varphi, k)$ are the first and second elliptical integrals to the modulus k with

$$k = \sqrt{1-(b/c)^2}\quad,\ \varphi = \arcsin\sqrt{\frac{c^2-x^2}{c^2-b^2}} \tag{20}$$

and $\mathbf{K}(k)$, $\mathbf{E}(k)$ are the complete elliptical integrals. In this context, it should be mentioned that in Ref. 11 the elliptical integral $\mathbf{K}$ is missing in the denominator of eqn (19). Equation (19) represents the displacement field for $\Delta h = 0$. In order to satisfy the constant displacements $\Delta h > 0$ in $-b < x < b$, we have to add the displacement field for a parallel rigid wedge of thickness $2\Delta h$ within $-b < x < b$. In order to avoid a separation of the contact surfaces we assume the wedge to be welded with the surrounding material along the interfaces. The displacements are also given in handbooks (e.g. Ref. 11). It holds

$$\delta_2(x) = \frac{F(\varphi,k)}{\boldsymbol{K}(k)}\Delta h \tag{21}$$

and, finally, the total solution for the displacements is given by

$$\delta(x) = \frac{2c\,\sigma_{\mathrm{appl}}}{E'\boldsymbol{K}(k)}\left[\boldsymbol{K}(k)\,E(\varphi,k) - \boldsymbol{E}(k)\,F(\varphi,k)\right] + \frac{F(\varphi,k)}{\boldsymbol{K}(k)}\Delta h \tag{22}$$

The crack opening displacement field resulting from eqn (22) is shown in Fig. 5.

3.2 Calculation of stresses in the bridging element

The corresponding stresses $\sigma(x)$ in the grain can be calculated numerically with eqn (18). In order to solve eqn (18), we will first calculate as a partial problem the stress distribution for a crack of length $2c$ which is opened by a parallel wedge of length $2b$ and thickness Δh (see Fig. 6). The Westergaard stress function for this problem is given in Ref. 11 as

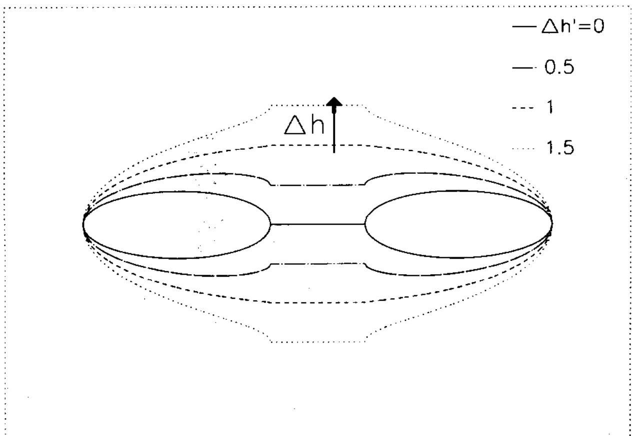

Fig. 5. Bridged crack. Displacements calculated with eqn (22), $b/c = 0{\cdot}2$ and σ_{appl} = constant, $\Delta h' = E'\Delta h/(2\sigma_{\mathrm{appl}}c)$.

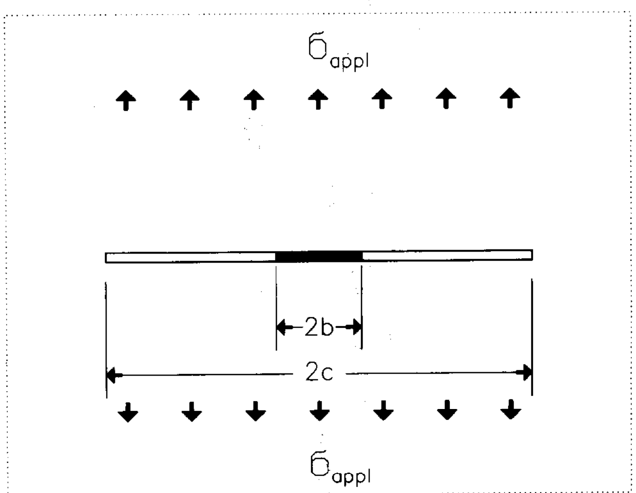

Fig. 6. Partial crack problem. Case 2: single crack opened by a wedge of constant thickness.

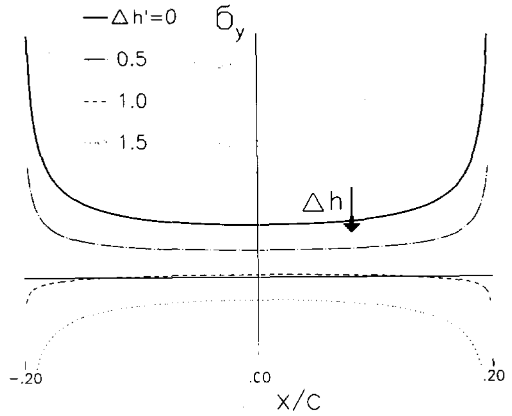

Fig. 7. Stresses in the bridging grain. Stresses calculated with eqn (18), $b/c = 0{\cdot}2$, σ_{appl} = const., $\Delta h' = E'\Delta h/(2\sigma_{appl}c)$.

$$Z(z) = \frac{E'h\,c}{2K(k)}\,\frac{1}{\sqrt{z^2-c^2}\,\sqrt{z^2-b^2}}, \qquad k = \sqrt{1-(b/c)^2} \tag{23}$$

from which the normal stress σ_y results by

$$\sigma_y = \mathrm{Re}\{Z(z)\} - y\,Im\{Z'(z)\} \tag{24}$$

For $y = 0$ one obtains

$$\sigma_y = \mathrm{Re}\{Z(z)\} \rightarrow \qquad \sigma_y = \frac{E'\Delta h\,c}{2K(k)}\,\frac{1}{\sqrt{c^2-x^2}\,\sqrt{b^2-x^2}} \tag{25}$$

For the pair of collinear cracks — which result for $\Delta h = 0$ — the stresses in the range $-b \le x \le b$ caused by the remote applied stress σ_{app} are (*see* Ref. 12)

$$\sigma_y = \frac{\sigma_{appl}}{K(k)}\,\frac{c^2E(k) - x^2K(k)}{\sqrt{(c^2-x^2)(b^2-x^2)}} \tag{26}$$

Superposition of the two partial crack problems yields

$$\sigma_y = \frac{1}{K(k)}\,\frac{\sigma_{appl}[c^2E(k) - x^2K(k)] - c\Delta hE'/2}{\sqrt{(c^2-x^2)(b^2-x^2)}} \tag{27}$$

The total force P carried by the bridging element is then

$$P = 2\int_0^b \sigma_y\,dx = 2\sigma_{appl}c[2E(k') - K(k')] - E'\Delta h \tag{28}$$

$$k' = \sqrt{1-k^2} = b/c \tag{29}$$

3.3 Load–displacement curve

The total volume resulting from the displacements

$$V = 4b\Delta h = 4\int_{x=b}^{x=c} \delta(x)\,dx \tag{30}$$

is a measure of the externally recorded loading-point displacements. From eqns (11) and (28) we find the applied stress at which the maximum friction force F_0 is reached

$$\sigma_{appl,0} = \frac{\mu F_0}{2c[2E(k') - K(k')]} \tag{31}$$

The volume at $\sigma_{appl} = \sigma_{appl,0}$ is

$$V_0 = \frac{8c\sigma_{appl,0}}{E'K(k)}\left[K(k)\int_b^c E(\varphi, k)\,dx - E(k)\int_b^c F(\varphi, k)\,dx\right] \tag{32}$$

For stresses below this limit the volume is

$$V = V_0\,\frac{\sigma_{appl}}{\sigma_{appl,0}} \tag{33}$$

and for higher stresses applied one obtains

$$V = V_0\,\frac{\sigma_{appl}}{\sigma_{appl,0}} + 4b\Delta h + \frac{4\Delta h}{K(k)}\int_b^c F(\varphi, k)\,dx \tag{34}$$

with Δh given as

$$\Delta h = h\,\frac{2E(k') - K(k')}{h' - [2E(k') - K(k')]}\left(\frac{\sigma_{appl}}{\sigma_{appl,0}} - 1\right) \tag{35}$$

$$h' = \frac{hE'}{2c\sigma_{appl,0}} \tag{36}$$

The volume — standing for the remote displacement at a given point — as a function of the applied remote stress is shown in Fig. 8. We can identify three regions:

1. For $\sigma_{appl} \le \sigma_{appl,0}$ the displacements are proportional to the applied load, as expressed by eqn (33).
2. At $\sigma_{appl,0}$ the applied stress overcomes the friction forces μF_0. For $\sigma_{appl,0} < \sigma_{appl} \le \sigma_{appl,max}$ the increase in displacements is steeper than in the range $\sigma_{appl} < \sigma_{appl,0}$.

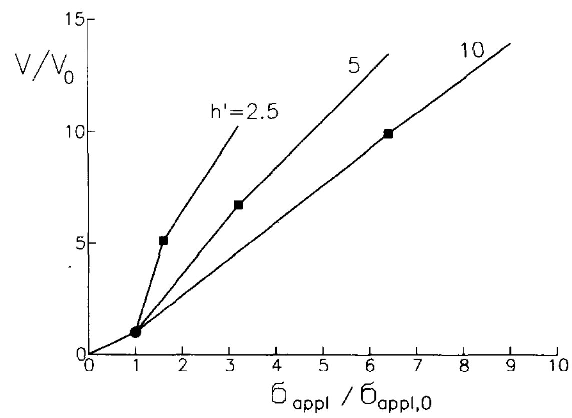

Fig. 8. Volume of the opened crack. Volume of the opened crack as a measure for the loading-point displacements, geometrical data: specimens thickness = 1 (i.e. crack opening area = crack opening volume), $b/c = 0{\cdot}2$, different values of h' as defined by eqn (36).

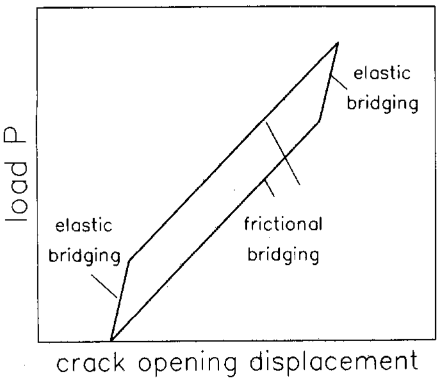

Fig. 9. COD-behaviour. Applied load, P, versus crack opening displacement curves for Al_2O_3 obtained by Dauskardt[9] (schematic).

3. At $\sigma_{appl,max}$ the bridging element is completely pulled out, equivalent to $\Delta h = h$,

$$\frac{\sigma_{appl,max}}{\sigma_{appl,0}} = \frac{h'}{2\boldsymbol{E}(k') - \boldsymbol{K}(k')} \tag{37}$$

and the subsequent curve follows according to

$$V = \frac{\sigma_{appl}}{\sigma_{appl,max}} = V_{appl,max} \tag{38}$$

Dauskardt[9] reports load–COD-curves which are very similar to those represented in Fig. 8. A typical P–COD-curve is schematically shown in Fig. 9 for one cycle of a cyclic test. Dauskardt calls the first steep part (corresponding to the initial flat parts of Fig. 8) 'elastic bridging' and the following phase 'frictional bridging'. Having in mind the COD-calculations made in this section, we can interpret the displacements during *elastic bridging* as the displacements occurring in the crack regions outside the actual bridging element (no elastic strain of the bridging element itself). Obviously, the displacements in Ref. 9 were not large enough ($K_I = K_{Ic}$ may be reached before) to exhibit the third part of the curve, i.e. the unbridged state.

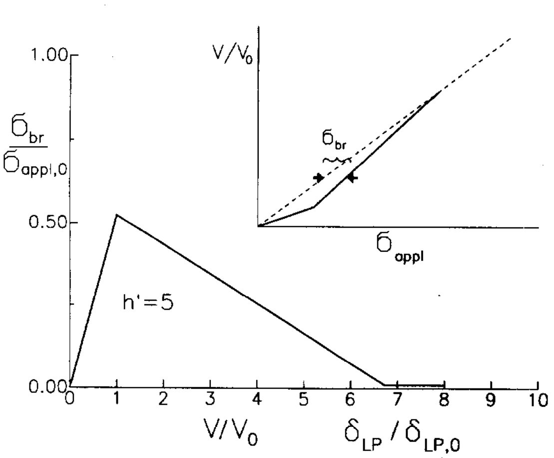

Fig. 10. Bridging stress relation. Bridging stress resulting from Fig. 8.

The bridging stresses result from the difference between the curve plotted in Fig. 8 and that curve which is obtained by prolongation of the line for $\sigma_{appl} \geq \sigma_{appl,max}$ to the origin (representing the completely unbridged state) as symbolised by the insert in Fig. 10. Considering the statistical distribution of the bridging-element lengths h, one obtains a smoother curve. If δ_{c1} is the displacement corresponding to $\sigma_{appl,0}$ and δ_c is the displacement at $\sigma_{appl.max}$, we can write the local bridging stresses as

$$\frac{\sigma}{\sigma_0} \begin{cases} \delta/\delta_{c1} & \text{for } \delta < \delta_{c1} \\ \dfrac{\delta_c - \delta}{\delta_c - \delta_{c1}} & \text{for } \delta_{c1} < \delta < \delta_c \\ 0 & \text{for } \delta < \delta_c \end{cases} \tag{39}$$

In the most general case one may consider the two typical displacements to be distributed independent of each other. But since the maximum friction force F_o characterising the onset of sliding, $\delta = \delta_{c1}$, is proportional to the length h of the bridging element and also the characteristic displacement of complete pull-out is identical to h, it is sufficient to consider the distribution of δ_c by introducing the ratio

$$\lambda = \delta_c/\delta_{c1} = \text{constant} \tag{40}$$

Replacing δ_{c1} in eqn (39) by $\delta_c\ \lambda$ and introducing this local bridging relation into eqn (3) yields for a Γ-distributed δ_c according to eqn (2) the averaged bridging relation

$$\sigma_{br} = \sigma_0 \frac{\lambda}{\lambda - 1} [\exp(-\delta/\delta_0) - \exp(-\lambda\ \delta/\delta_0)] \tag{41}$$

In Ref. 13 the authors used a Morse-like bridging relation

$$\sigma_{br} = \sigma_0 [\exp(-\delta/\delta_0) - \exp(-2\ \delta/\delta_0)] \tag{42}$$

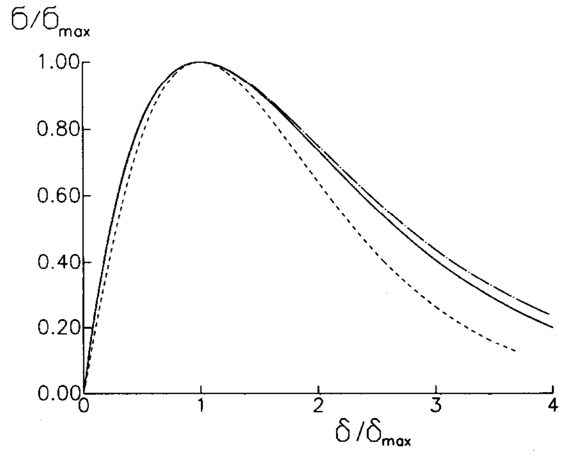

Fig. 11. Comparison of bridging stress relations. Solid curve: eqr (7), dashed curve: eqn (9), dash-dotted curve: eqn (42); δ_{max} is that displacement at which the stress reaches its maximum value.

which is a special case of eqn (41) with $\lambda = 2$. A comparison between the bridging relations described by eqns (7), (9), and (42) is given in Fig. 11.

4 Summary

Bridging stresses in ceramic materials are responsible for the R–curve behaviour. They are generated by crack surface interactions in the wake of a propagating crack and can be caused by friction of sliding grains or by elastic interactions where the crack surface contact behaves like a spring. In this paper, relations for the average bridging stresses as a function of the actual crack opening displacement are proposed and a model is discussed which allows to combine the two effects leading to 'elastic bridging' and 'frictional bridging' as observed by Dauskardt.[9]

The model yields a relation between the bridging stresses and the crack opening displacements. The three free parameters σ_0, λ and δ_0 may be determined

- by direct measurements of the bridging stresses in tensile tests,[14]
- from load–displacement curves as given by Dauskardt,[9]
- by fitting the bridging relation to measured R–curves.

References

1. Steinbrech, R. & Schmenkel, O., Crack-resistance curves for surface cracks in alumina, Comm., *J. Amer. Ceram. Soc.*, **71** 1988 C271.
2. Fett, T. & Munz, D., Evaluation of R–curve effects in ceramics, *J. Mater. Sci.*, **28** 1993 742–52.
3. Knehans, R. & Steinbrech, R. W., Memory effect of crack resistance during slow crack growth in notched Al_2O_3 bend specimens. *J. Mater. Sci. Letters*, **1** (1982) 327–9.
4. Steinbrech, R. W., Knehans, R. & Schaarwächter, W., Increase of crack resistance during slow crack growth in Al_2O_3 bend specimens. *J. Mater. Sci.*, **18** (1983) 265–70.
5. Frei, H. & Grathwohl, G., New test methods for engineering ceramics — in situ microscopy investigation, *Ceramic Forum International, cfi*, **67** 1991 27–35.
6. Rödel, J., Kelly, J. F. & Lawn, B. R., In situ measurements of bridged crack interfaces in the scanning electron microscope. *J. Amer. Ceram. Soc.*, **73** (1990) 3313–8.
7. Mai, Y. & Lawn, B. R., Crack–interface grain bridging as a fracture resistance mechanism in ceramics: II. Theoretical fracture mechanics mode, *J. Amer. Ceram. Soc.*, **70** (1987) 298.
8. Rombach, M., Rißachstum in Si_3N_4, Diplomarbeit, Universität Freiburg, 1992.
9. Dauskardt, R. H., Cyclic fatigue-crack growth in grain bridging ceramics, *J. of Engng. Mater. and Techn.*, **115** (1993) 244–51.
10. Fett, T., Mattheck, C. & Munz, D., On the calculation of crack opening displacement from the stress intensity factor, *Engng. Fract. Mech.*, **27** (1987) 697–715.
11. Tada, H., Paris, P. C. & Irwin, G. R., *The stress analysis of cracks handbook*, Del Research Corporation (1986).
12. Hahn, H. G., Bruchmechanik, B. G. Teubner, Stuttgart 1976.
13. Fett, T. & Munz, D., Influence of crack-surface interactions on stress intensity factor in ceramics, *J. Mater. Sci. Letters*, **9** (1990) 1403–6.
14. Hay, J. C. & White, K. W., Crack face bridging tractions in monolitic spinel. In *Fracture Mechanics of Ceramics* Vol. 9 (1992) 265–76.